CHEMMEDCHEM

DOI: 10.1002/cmdc.201000106

Rational Design, Synthesis, and DNA Binding Properties of Novel Sequence-Selective Peptidyl Congeners of Ametantrone

Alessandra Gianoncelli,[a] Serena Basili,[a] Matteo Scalabrin,[a] Alice Sosic,[a] Stefano Moro,[a] Giuseppe Zagotto,[a] Manlio Palumbo,[a] Nohad Gresh,[b] and Barbara Gatto*[a]

Natural and synthetic compounds characterized by an anthraquinone nucleus represent an important class of anti-neoplastic agents, the mechanism of action of which is related to intercalation into DNA. Ametantrone (AM) is a synthetic 9,10-anthracenedione bearing two (hydroxyethylamino)ethylamino residues at positions 1 and 4; along with other anthraquinones and anthracyclines, it shares a polycyclic intercalating moiety and charged side chains that stabilize DNA binding. All these drugs elicit adverse side effects, which represent a challenge for antitumor chemotherapy. In the present work the structure of AM was augmented with appropriate groups that target well-defined base pairs in the major groove. These should endow AM with DNA sequence selectivity. We describe the rationale for the synthesis and the evaluation of activity of a new series of compounds in which the planar anthraquinone is conjugated at positions 1 and 4 through the side chains of AM or other bioisosteric linkers to appropriate dipeptides. The designed novel AM derivatives were shown to selectively stabilize two oligonucleotide duplexes that both have a palindromic GC-rich hexanucleotide core, but their stabilizing effects on a random DNA sequence was negligible. In the case of the most effective compound, the 1,4-bis-[Gly-(L-Lys)] derivative of AM, the experimental results confirm the predictions of earlier theoretical computations. In contrast, AM had equal stabilizing effects on all three sequences and showed no preferential binding. This novel peptide derivative can be classified as a strong binder regarding the sequences that it selectively targets, possibly opening the exploitation of less cytotoxic conjugates of AM to the targeted treatment of oncological and viral diseases.

Introduction

Anthraquinones have been used as efficient compounds in treating several kinds of cancers. The discovery of the antitumor activity of 1,4-bis[(aminoalkyl)amino]anthracene-9,10-diones such as ametantrone (AM) and mitoxantrone (MX) (Figure 1) has led to numerous studies on their tumoricidal mechanisms and on those of their congeners.[1] They are classic intercalating agents that accumulate in the nucleus, where they poison topoisomerase II, and there is good evidence that the impaired topoisomerase II (i.e., a stabilized DNA–topoisomerase II cleavable complex) contributes to the cytotoxic effect.[2] In addition, it has also been demonstrated that the oxidation products of MX, catalyzed by horseradish peroxidase, form a covalent complex with DNA in vitro,[3] and similar drug–DNA adducts were also detected when the drug was oxidized in vitro by the human enzyme myeloperoxidase.[4]

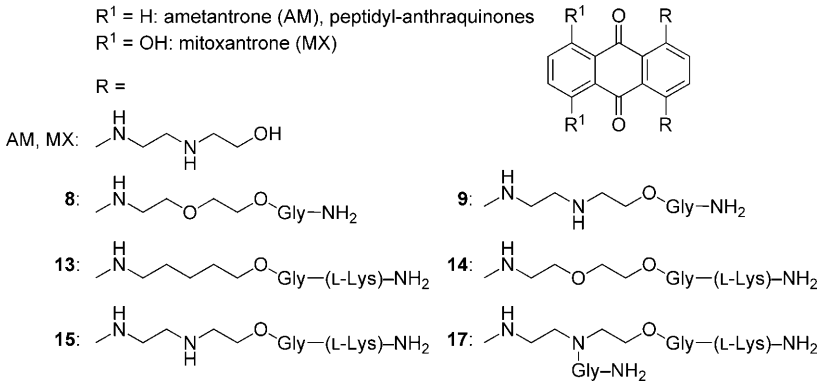

Figure 1. Structures of ametantrone (**3**), mitoxantrone, and tested peptidyl-anthraquinones.

The anthraquinone ring system enables intercalation between base pairs of DNA in the B conformation.[5] In MX and AM the nucleus is intercalated along a direction perpendicular

[a] *Dr. A. Gianoncelli, Dr. S. Basili, Dr. M. Scalabrin, Dr. A. Sosic, Prof. S. Moro, Prof. G. Zagotto, Prof. M. Palumbo, Prof. B. Gatto*
Dipartimento di Scienze Farmaceutiche, Università di Padova
Via Marzolo 5, 35131 Padova (Italy)
Fax: 0039-049-8275366
E-mail: barbara.gatto@unipd.it

[b] *Prof. N. Gresh*
Laboratoire de Pharmacochimie Moléculaire et Cellulaire
U648 INSERM, UFR Biomédicale
Université Paris Descartes, Paris (France)

Supporting information for this article is available on the WWW under http://dx.doi.org/10.1002/cmdc.201000106.

to the long axis of the base pairs. This places the two arms, located at positions 1 and 4, in the major groove of DNA and in symmetrical antiparallel arrangements, each arm interacting with a distinct strand.[6] Although AM is approximately 10-fold less potent in vivo and 100-fold less potent in vitro than MX,[7] it exhibits a lower genotoxicity.[8] The chemical and biological activity exhibited by anthraquinone compounds are greatly affected by the different substituents of the planar ring system.[1,9] Side chains bear usually one or two positive charges to establish an electrostatic interaction with the phosphate backbone of the polynucleotide.

Our group has explored the changes in the physicochemical and biological properties of substituted anthraquinones in which peptide chains are connected through an amide bond to the planar ring.[10–16] A peptide sequence linked to a pharmacophore group could, if properly selected and substituted, confer drug specificity. In fact, it is well known that precise recognition of defined DNA sequences in biological systems is mediated by enzymes and proteins that have appropriate structural motives. Indeed, one of the major drawbacks of DNA-directed anti-neoplastic agents is their inability to selectively target cancer cells. Therefore the introduction, into presently available drugs, of specific recognition elements for mutated oncogenes elements should represent a basic advance in cancer chemotherapy.

The present study is part of our endeavor to design oligopeptide-conjugated intercalator molecules that target well-defined DNA sequences in the major groove.[17–20] On the basis of computational studies, anthraquinone derivatives were designed, and their binding energies with $d(GGCGCC)_2$ were compared to those with the other concurrent palindromic sequences containing the CG step. The $d(GGCGCC)_2$ sequence, a mutational hot spot in DNA, is located in several oncogenes and is also part of the primer binding site (PBS) of the long terminal repeat (LTR) of the HIV-1 retrovirus that is necessary for the initial steps of reverse transcriptase (RT)-mediated cDNA synthesis.[19,21,22] Therefore, it also represents an important target for the design of novel antiviral drugs.

To verify these modeling predictions experimentally,[17,18] we synthesized and tested the series of compounds depicted in Figure 1. The substituents are linked to the anthraquinone by esterification of the two arms of AM (**3**) with Gly or Gly-(L-Lys) (compounds **9** and **15**), in which **15** represents the peptidyl-AM predicted to exhibit sequence-selective properties. Extending the arms upon passing from Gly to Gly-Lys should enable the cationic Lys side chains to bind to electron-rich O6/N7 sites with G bases upstream of the intercalation site.[18] An important feature of these derivatives is the presence of a free nitrogen in the lateral chains (N-series), **17** was therefore synthesized as a control. Earlier studies demonstrated that such a nitrogen plays an important role because no activity is observed when it is replaced by a methylene group or another atom.[23] Further appropriate controls for our designed peptidyl-derivative of AM bear different linkers between the planar nucleus and the peptide chains (-CH_2- and -O- series), exemplified respectively by compounds **13** and **14**. Of the Gly series, compounds **8** and **9** were included as controls, whereas the alkyl isostere was synthesized (**7** in Scheme 3 below) but could not be tested due to its limited water solubility.

We performed a DNA-unwinding assay to evaluate if the new derivatives bind to DNA as intercalators, and whether intercalation parallels the ability to inhibit human topoisomerase II. By using a fluorescence-quenching assay (FQA) coupled to thermal denaturation of short double-stranded (ds) oligonucleotides labeled with appropriate fluorescence/quenching probes we aimed to demonstrate whether the novel derivatives display the desired sequence-specific recognition. Our earlier theoretical studies predicted that the peptide backbones of the two arms of the anthraquinone nucleus should adopt an antiparallel β-sheet arrangement, enabling each arm to interact with one distinct strand.[17,18] Their symmetrical disposition with respect to the chromophore is a reflection of the palindromic nature of targeted sequences $d(GGCGCC)_2$ and $d(CCCGGG)_2$ that were chosen for our studies.

Furthermore, an accurate structural and dynamical description of peptidyl anthraquinone complexes in aqueous solution, which would help to understand the molecular basis of ligand–DNA recognition can be obtained through molecular dynamics (MD) simulations. Here we make use of the Amber force field to investigate through MD simulation the dynamical and stability properties of the novel peptidyl anthraquinone complexes with the aim to verify earlier predictions and rationalize the observed structure–activity relationship.

Results and Discussion

Chemistry

To obtain the ametantrone isosteres **1** and **2** we treated leucoquinizarin (**L**) with two equivalents of amine to get the Schiff bases, which were then isomerized and oxidized by air as shown in Scheme 1.

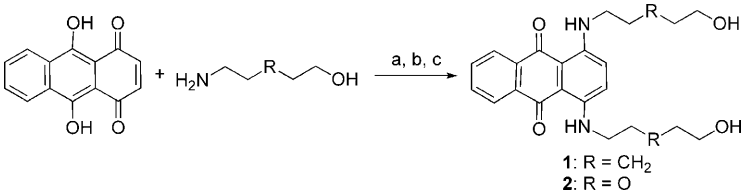

Scheme 1. Reagents and conditions: a) $Na_2S_2O_4$, N_2, H_2O, 70–80 °C; b) $NH_2(CH_2)_2X$-$(CH_2)_2OH$, N_2, H_2O, 100 °C, overnight; c) O_2, H_2O, 25 °C, 6 h.

For the synthesis of ametantrone (**3**) we used a reported procedure by starting from 1,4-difluoroanthraquinone (Scheme 2 A)[1] because the former procedure with *N*-(2-hydroxyethyl)ethylenediamine and leucoquinizarin gave the cyclization compound 1,2,3,4-tetrahydro-4-(2-hydroxyethyl)-6-[{2-[(2-hydroxyethyl)amino]ethyl}amino]naphtho[2,3-*f*]quinoxaline-7,12-dione **3**′ (Scheme 2 B).[24]

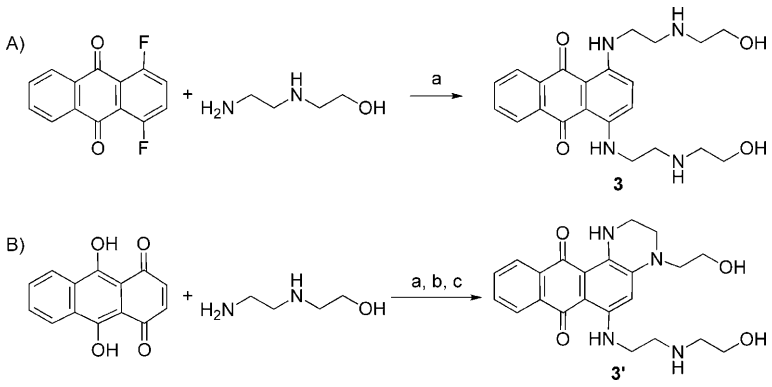

Scheme 2. A) Reagents and conditions: a) DMSO, room temperature, 96 h. B) Reagents and conditions: a) $Na_2S_2O_4$, N_2, H_2O, 70–80 °C; b) $NH_2(CH_2)_2NH(CH_2)_2OH$, N_2, H_2O, 100 °C, overnight; c) O_2, H_2O, 25 °C, 6 h.

Then the alcoholic groups of both chains in **1**–**3** were esterified with Boc-Gly-OH, and the Gly was deprotected with 90% trifluoroacetic acid (TFA) to give compounds **7**–**9** as shown in Scheme 3.

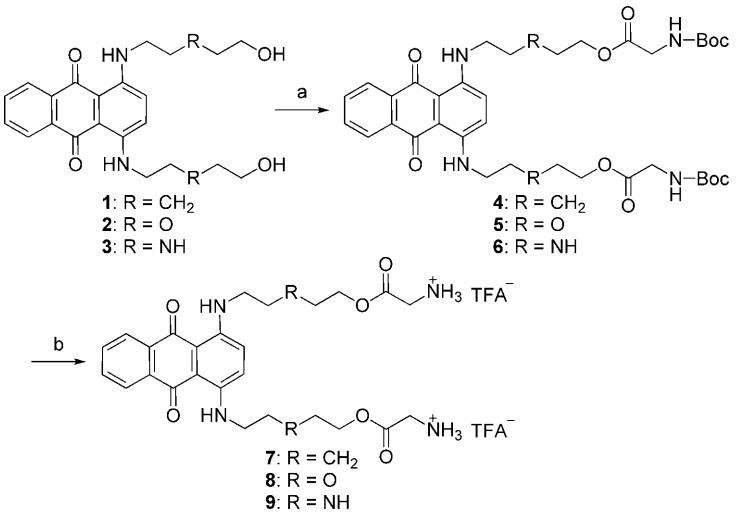

Scheme 3. Reagents and conditions: a) DCC, DMAP, Boc-Gly-OH, THF, room temperature, 16 h, $Ar_{(g)}$; b) TFA 90% 1 h, Et_2O.

The reaction of intermediates **7**–**9** with Boc-Lys(Boc)-OH and the successive deprotection of all amino groups with 90% TFA gave compounds **13**–**15**, as shown in Scheme 4.

Upon treating Boc-Gly-OH with the ametantrone side chain, both of the secondary aliphatic amines and both of the primary alcohols were acylated to give the tetrasubstituted compound **17** (Scheme 5).

Peptidyl-anthraquinones are DNA intercalators

The electrophoresis mobility of different topological DNA forms offers an easy way to analyze the intercalation potency of the novel compounds. In this work the changes in topological properties of pBR322 plasmid after incubation with peptidyl-anthraquinones are analyzed by their different electrophoretic mobilities. DNA migration reflects the extent of intercalation due to the complexed ligand and also the persistence of the complex in an electric field. AM (**3**), used as a positive control, was found to have the strongest intercalation properties because gel retardation was evident already at 10 μM (Figure 2).

The novel peptidyl-anthraquinones in the nitrogen series have weaker unwinding properties: **9** and **15** show an appreciable effect only at 10-fold higher concentrations, whereas unwinding of plasmid DNA is more pronounced for **17** and shows a good correlation between DNA mobility and concentration. The bioisostere control **8** seems not to appreciably modify the topological state of plasmid pBR322 at any concentration tested, and **14** demonstrates a weak unwinding at the highest concentration taken. The alkyl isostere **13** shows DNA retardation at 10 μM, but at 100 μM ethidium staining of the lane is reduced, and DNA is precipitated in the loading well (Figure 2).

Peptidyl conjugates of AM exhibit sequence--selective DNA binding

Having established that the novel peptidyl-anthraquinones derived from AM are intercalators that are able to unwind DNA, it was essential to obtain information on their DNA sequence-selective binding. Therefore, we resorted to fluorescence-quenching assays (FQA) to analyze the melting profiles of three different double-stranded oligonucleotides upon peptidyl-anthraquinone addition. All three oligos are 18 base pairs long. The first sequence, used as a control, has a random alternation of bases (denoted as random oligo).[25] The two other ones have core palindromic GC-rich hexanucleotides, namely, CCCGGG (Z1) or GGCGCC (Z2). Their choice was made on the basis of molecular modeling,[18] which predicted these as the major targets for the Gly-Lys derivative **15**.

FQA was run with FAM and DAB probes, as described.[25] Briefly, forward strand oligonucleotides were labeled at their 5′ ends with FAM, whereas the DAB quencher was labeled at the 3′ end of the complementary sequence. The double-stranded oligonucleotide that resulted when the two complementary strands were annealed is a blunt-ended hybrid that places FAM and DAB so close together that contact quenching occurs. Indeed, neither the peptidyl-anthraquinones, nor the DAB-labeled oligonucleotides, nor the hybridized blunt-end oligo showed an appreciable fluorescence when excited at 494 nm at room temperature, but the free FAM-labeled oligonucleotides under the same conditions showed an appreciable emission at 520 nm. As melting of the hybridized oligo duplexes takes place upon temperature increase, the FAM-labeled oligonucleotide is released from the quenching effect and its fluorescent signal increases due to the increasing distance between the two probes (not shown).

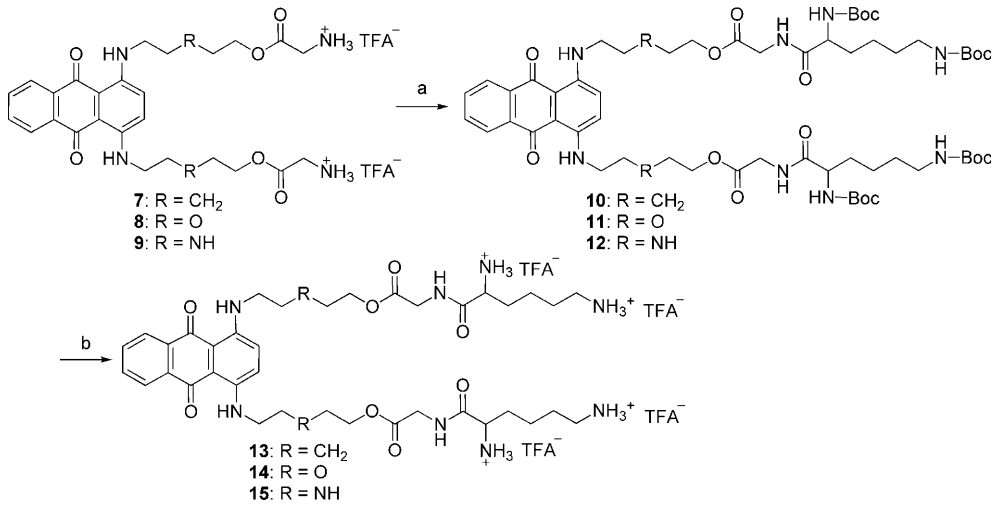

Scheme 4. Reagents and conditions: a) Boc-Lys(Boc)-OSu, DMF, CH_2Cl_2, Et_3N, room temperature, 16 h, $Ar_{(g)}$; b) TFA 90% 1 h, Et_2O.

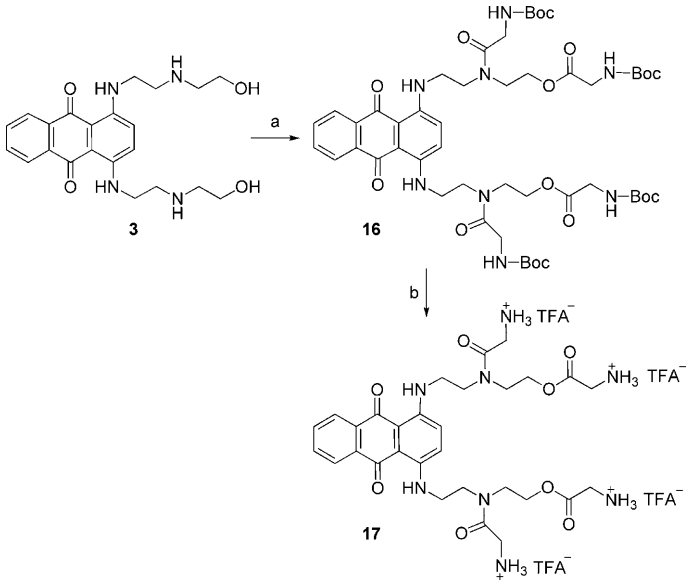

Scheme 5. Reagents and conditions: a) DCC, DMAP, Boc-Gly-OH, THF, room temperature, 16 h, $Ar_{(g)}$; b) TFA 90% 1 h, Et_2O.

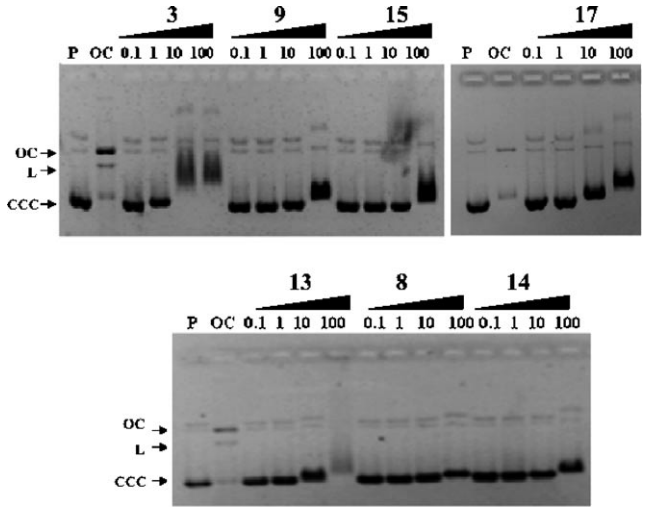

Figure 2. DNA-unwinding assay. Negatively supercoiled plasmid at defined conditions migrates with the highest mobility (covalently closed circular DNA, CCC). Increasing quantities of intercalating agents provoke unwinding of supercoiled forms of DNA, and hence variation in the hydrodynamic volume of DNA. This effect is visualized by retardation in the electrophoretic migration of supercoiled plasmid. P = 0.25 μg supercoiled pBR322; OC = 0.1 μg plasmid in open circular form obtained by limited DNase action; L = linearized pBR22. Indicated compound concentrations are expressed as micromolar. Electrophoresis [1% agarose gel in TBE 1× (89 mM Tris, 89 mM boric acid, 2 mM EDTA, pH 8.0)] was run overnight 15 mV cm^{-1}, and the gel was stained with ethidium bromide.

The T_m of each oligo pair was determined as the temperature value at which the melting profile (fluorescence vs. temperature) presents a flex point. We then measured the T_m of the three different double-stranded oligonucleotides in the presence of the AM control (**3**) and of each peptidyl-anthraquinone tested at 1, 10, and 100 μM concentration, and calculated the ΔT_m values reported in Table 1.

Melting experiments, although consistent with DNA-unwinding studies, indicate that the peptidyl-anthraquinones behave in contrasting ways upon binding to the random and the two sequences having GC-rich core palindromes. This is evidenced in Figure 3, which reports the relative stabilization of each oligo duplex at the tested peptidyl-anthraquinones/DNA ratios.

Indeed, **3**, **13**, and **17** act as nonselective binders because they stabilize the three sequences by the same amount. Compounds **8** and **14** are poor binders in all cases, whereas **15** and, to a lesser extent, **9** emerge as sequence-selective binders.

Our experimental results confirm, as predicted, that the free nitrogen in the linker of **15** and, to a lesser extent, **9** is necessary for long-range specificity when the peptide is conjugated to the ametantrone nucleus. Indeed, **17** and **9** further illustrate the contribution of the free nitrogen: in the former derivative, an additional Gly is conjugated through an amide bond to the nitrogen in the lateral chain: it is evident that when the side chain nitrogen is not free (compound **17**) sequence-specific DNA binding of **9** is lost.

Regarding the melting analysis, in the case of compound **13** with Z2 at 100 μM we never observed fluorescence signals at any temperature, which is likely due to the precipitation of the oligo in the capillary that was used for the melting analysis. Therefore, the ΔT_m determination for this particular sample could not be performed. Precipitation of DNA by a high concentration of **13** was observed also in the unwinding experiments, and further confirmed by CD spectroscopy (see the

Table 1. DNA binding of peptidyl-anthraquinones expressed as a function of ΔT_m.

Compd	Oligo[a]	ΔT_m [°C] 1 μM	10 μM	100 μM
	Random[b]	1.26 ± 0.80	5.54 ± 0.96	14.60 ± 1.37
3	Z1[c]	1.08 ± 0.07	5.85 ± 0.51	16.66 ± 0.65
	Z2[d]	1.24 ± 0.19	6.11 ± 1.22	15.45 ± 0.13
	Random	0.00	0.22 ± 0.21	2.40 ± 0.33
8	Z1	0.00	0.00	1.74 ± 0.53
	Z2	0.00	0.00	2.11 ± 0.41
	Random	0.00	0.18 ± 0.16	2.80 ± 0.86
9	Z1	0.00	2.98 ± 0.04	10.74 ± 0.60
	Z2	0.00	2.48 ± 0.33	9.84 ± 0.29
	Random	0.00	0.35 ± 0.26	13.09 ± 1.25
13	Z1	0.00	0.67 ± 0.59	14.29 ± 0.69
	Z2	0.00	0.73 ± 0.48	ND[e]
	Random	0.00	0.00	2.31 ± 1.01
14	Z1	0.00	0.00	4.19 ± 0.31
	Z2	0.00	0.00	3.52 ± 0.40
	Random	0.00	0.41 ± 0.76	3.70 ± 0.77
15	Z1	0.00	4.02 ± 0.04	16.05 ± 0.13
	Z2	0.00	3.26 ± 0.33	16.04 ± 0.64
	Random	0.24 ± 0.17	2.21 ± 0.21	8.23 ± 0.25
17	Z1	0.00	2.69 ± 0.11	9.10 ± 1.24
	Z2	0.00	2.38 ± 0.33	8.78 ± 0.28

[a] Annealed ds oligo (0.25 μM) in Tris 10 mM, EDTA 1 mM, NaCl 20 mM, pH 7.5. [b] Random oligo $T_m = 48.07 \pm 0.71$ °C. [c] Z1 sequence (core: CCCGGG) $T_m = 45.95 \pm 0.14$ °C. [d] Z2 sequence (core: GGCGCC) $T_m = 48.34 \pm 0.40$ °C. [e] Not determined.

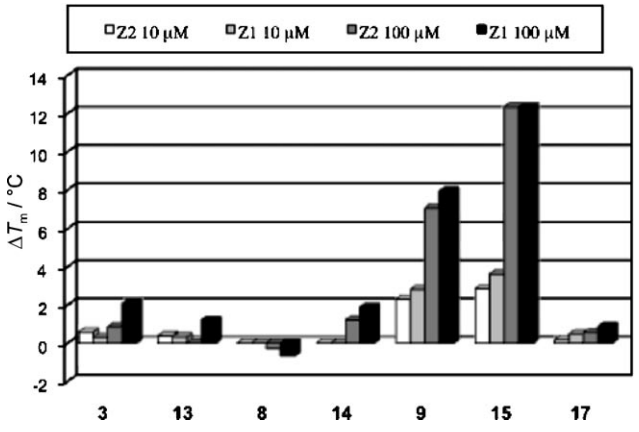

Figure 3. Sequence-specific recognition of AM-derived peptidyl-anthraquinones. Differential stabilization (ΔT) of the designed oligonucleotides (Z1 and Z2 core sequences) with reference to a random duplex sequence by 10 and 100 μM ligand. Annealed ds oligos were 0.25 μM in 10 mM Tris, 1 mM EDTA, 20 mM NaCl, pH 7.5. Data from FQA experiments reported in Table 1.

Supporting Information). This peculiar difference from its congeners **14** and **15** is clearly ascribable to the long alkyl linkers, which can interact with each other in solution as well as in the complex with DNA.

Molecular dynamics of DNA–14 and DNA–15 complexes

The conformational features of the sequence specific peptidyl-derivative **15** and of its non-sequence-specific isostere **14** in complex with the core hexameric sequence of Z2 oligo (respectively DNA–**15** and DNA–**14**) during the MD trajectory have been checked upon monitoring specific structural parameters as a function of time. The root-mean-square deviation (RMSD) calculated for all atoms of both complexes are reported in Figure 4. The deviation of the intercalative complex geometry from the initial conformation increases with time although over the whole trajectory the simulated decanucleotide duplex structures remain closer to that of canonical B-DNA. The RMSD from the average MD structure oscillates around 1.5 Å for the DNA–**15** complex and around 2.2 Å for the DNA–**14** complex. This indicates that both intercalative complexes are stabilized in a well-defined configuration during the simulation.

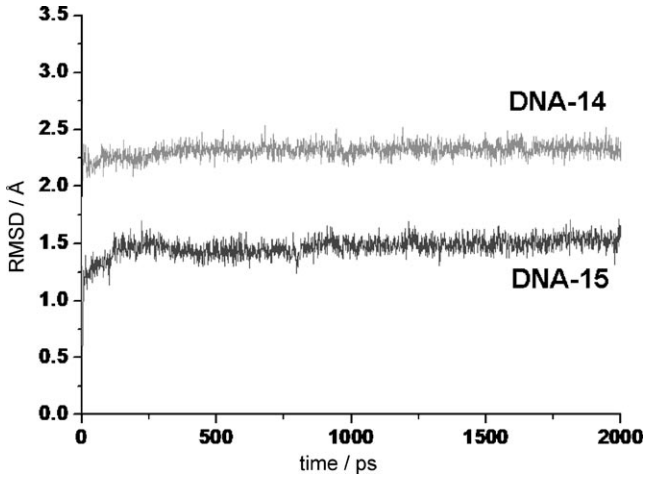

Figure 4. Root-mean-square atom positional deviations of complexes DNA–**14** and DNA–**15** (see labels) as a function of simulation time. The structures were superimposed and the RMSDs were calculated for all atoms excluding the first two and the last two base pairs.

The higher RMSD average value measured during the trajectory for the DNA–**14** complex can be explained by the loss of the electrostatic interactions that take place between the protonated secondary amine present in the linker of **15** and the adjacent DNA in the corresponding DNA–**15** complex (see Figure 5). In **14**, the secondary amine is replaced by an ether moiety.

The essential role of such an electrostatic interaction can also be evidenced by monitoring the interaction energy profile of the complexes of **14** and **15** during MD. As observed in Figure 6, the overall stability of the DNA–**15** complex is higher than that of the DNA–**14** complex due to its more favorable electrostatic energy contribution. For both complexes, on the other hand, on each strand the Lys side chain binds to the O6/N7 electron-rich atoms of two G bases upstream of the intercalation site, as shown in Figure 5. These electrostatic interactions increase the stability of both complexes.

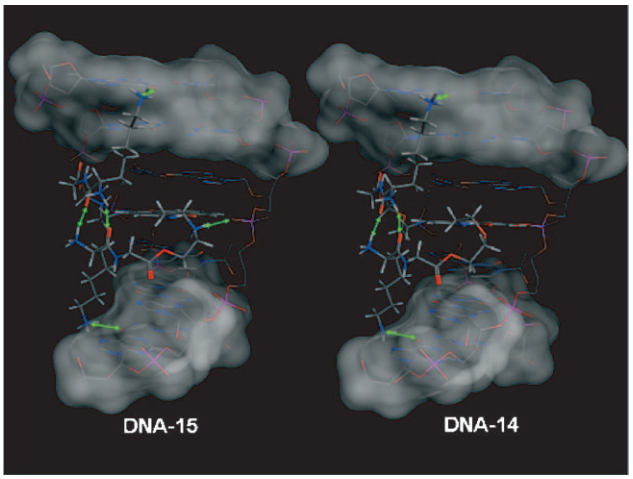

Figure 5. Structure of the binary complex of peptidyl-anthraquinones **14** (on the right) and **15** (on the left) with the target DNA sequence. All complexes are displayed from the side of the DNA longitudinal axes. DNA base pairs, above and below the intercalation site, are represented by the corresponding Connolly surface colored in light gray. Stabilizing interactions are indicated by green arrows.

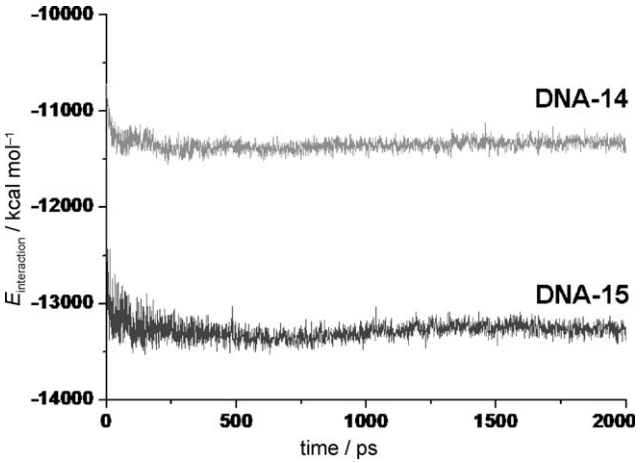

Figure 6. Interaction energies as a function of simulation time of the DNA duplex interacting with peptidyl-anthraquinones **14** and **15**.

The β-sheet-like motif of the two peptidyl tails of both **14** and **15** is also conserved. In fact, the double charge–dipole interactions mediated by the two lysines seem to guarantee this stable conformation over the entire 2 ns course of simulation. It is also gratifying to observe that such a motif, which had been predicted earlier on the basis of simpler energy minimizations,[17,18] could be retained in the course of the 2 ns simulation.

Biological evaluation of peptidyl-anthraquinones

We have shown that a simple dipeptide can be conjugated to the nucleus of a known intercalator to direct it to sequence specific recognition of DNA. Because AM is a cytotoxic drug, we investigated whether its cell toxicity could be affected by peptide conjugation. The data reported in Table 2 show in fact

Table 2. Cell toxicities and log *P* values of peptidyl-anthraquinones.

Compd	EC_{50} [μM][a]			log *P*[b]
	HL60	LoVo	HeLa	
3	0.27 ± 0.1	1.50 ± 0.1	0.90 ± 0.11	0.36 ± 0.07
8	30.0 ± 6.1	NA[c]	66.5 ± 14.3	1.30 ± 0.08
9	NA	96.0 ± 6.9	NA	−0.41 ± 0.13
13	27.7 ± 3.7	44.1 ± 1.6	83.2 ± 17.1	0.30 ± 0.15
14	NA	NA	NA	0.78 ± 0.11
15	43.5 ± 6.5	NA	NA	−2.65 ± 0.21
17	NA	NA	NA	−1.08 ± 0.05

[a] Determined at 72 h by MTT assay. [b] Determined experimentally at pH 7.4. [c] Not active ($EC_{50} \geq 100$ μM).

that the novel compounds are significantly less cytotoxic than AM (**3**) in all of the tested lines, namely the leukemia cell line HL60, the LoVo colon carcinoma cells, as well as the HeLa (cervical carcinoma), with leukemia cells being the most sensitive. Such a limited toxicity can be ascribed to an impaired permeation in cells due to the increased charge of the peptidyl conjugates, in particular in **15**, as we have observed for other highly charged derivatives.[26] Therefore, we similarly attempted to measure the uptake of the peptidyl-anthraquinones in the HL60 cells to verify this hypothesis. However, because the peptidyl-anthraquinones are not fluorescent, and their molar absorptivity at the absorbance maximum is low, the estimate of concentration was not precise enough to safely determine the amount of their uptake in HL60 cells. Hence, we experimentally measured their permeation coefficient to determine the relative lipophilicity of these highly charged derivatives and correlate them with the biological data. The results, shown in Table 2, indicate that all the peptidyl-derivatives of AM, namely **9**, **15**, and **17**, exhibit negative permeation coefficients, with the lysyl derivative **15** being the most hydrophilic of the series; this offers an explanation for the low cytotoxicity.

However, **15** exhibits a residual cell cytotoxicity in the leukemia cell line, whereas it is considered to be inactive ($EC_{50} \geq$ 100 μM) in the other tested cell lines. Isosteres and controls show different biological activity: in the series represented by **8** and **14** the less-charged derivative **8** has a limited cytotoxicity consistent with its lipophilic character, whereas its more charged Lys derivative **14**, the isostere of **15**, loses activity while retaining a good permeation coefficient. The other isostere, **13**, shows high permeation that, coupled to a good although nonselective DNA binding, allows it to retain cytotoxic properties.

Hence, the fraction of **15** able to reach and bind to specific DNA sequences might be able to elicit cell responses. Because AM can affect topoisomerase II (topo II) activity, we analyzed the activity of AM-derived peptidyl-anthraquinones toward the catalytic activity of this enzyme. Inhibition of pBR322 relaxation by topo II (Figure 7) performed with purified human enzyme under these experimental conditions was positive for **3** at 10 μM, whereas **15** showed inhibition only at the highest concentration (100 μM). This result is consistent with those of the unwinding experiments and rules out topo II as a primary target for AM-derived peptidyl-anthraquinones.

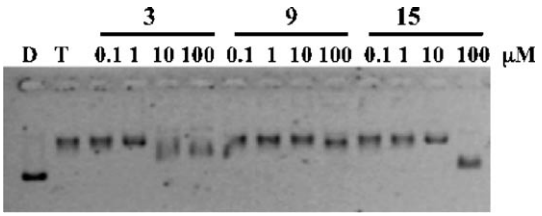

Figure 7. Human topoisomerase IIα relaxation assay. AM (**3**) and peptidyl-AM derivative concentrations used were 0.1, 1, 10, and 100 μM as indicated, and were incubated for 1 h at 37 °C with DNA and enzyme before stopping the reaction. D = 0.1 μg plasmid DNA; T = human topo IIα isoform (0.01 U). Electrophoresis [1% agarose gel in 89 mM Tris, 89 mM boric acid, 2 mM EDTA, pH 8.0] was run overnight 15 mV cm^{-1} and stained after the run with ethidium bromide.

Conclusions

The search for specificity is a critical challenge in pharmaceutical sciences. The ability to distinguish between healthy and malignant or infected cells, to prevent recognition of multiple targets, and avoid the onset of undesired effects, is a major incentive for the development of novel, effective drugs. Computational studies can be a very valuable asset toward the rational design of selective DNA binding ligands. In the present work, and on the basis of earlier computational studies, we investigated novel anthraquinone compounds derived from ametantrone, a well-studied antitumor compound. One of the novel derivatives was designed to target selectively the palindromic GC-rich sequences $(GGCGCC)_2$ and $(CCCGGG)_2$.

The change of topological forms of plasmid pBR322 upon compound addition (unwinding assay) enabled us to examine the intercalation properties of the new peptidyl-anthraquinones relative to the parent compound AM, and melting profiles coupled to FQA gave us information on sequence selectivity and allowed us to evaluate whether the peptidyl derivatives could selectively target the desired sequences.

Our new series of designed peptidyl-anthraquinones exhibit a flexible and basic linker: **15**, which bear a Gly-(L-Lys) dipeptide conjugated as a depsipeptide to the anthraquinone, is the most sequence selective of the whole series, in complete agreement with the theoretical predictions.[18] The two isostere controls that were synthesized and tested were **13** (alkyl linker) and **14** (ether linker), which conjugate the anthraquinone nucleus to the same Gly-(L-Lys) dipeptide. Compound **14** is a poor DNA binder in all cases, whereas the alkyl isostere **13** binds DNA without any sequence discrimination and causes precipitation as evidenced in unwinding and in FQA experiments, and confirmed in CD spectroscopy experiments.

MD analysis supports our binding data; interestingly, the peptidyl tails of **15** adopt a β-sheet conformation. This motif could be used as a scaffold to graft side chains at appropriate locations to target specific bases upstream of the intercalation site. DNA recognition in the major groove occurs in the majority of cases by proteins that adopt an α-helical conformation. There exist however precedents for proteins that bind to DNA in the major groove and adopt a β-sheet conformation, as in the case of the dimeric Arc repressor.[27,28]

The biological evaluation of the new compounds showed that the presence of the lysine-containing peptide in the AM-derived series, although necessary for sequence-specific DNA recognition, confers a decisively high hydrophilic character, impairing biological effects in the cell lines tested. However, the residual cytotoxicity exhibited by the highly charged compound **15** points to the possibility of exploiting appropriate delivery systems to circumvent cell permeation. Furthermore, in a new but promising line of research, the limited cytotoxic effect exhibited by the peptidyl-AM **15** coupled to its sequence preferences for the $d(GGCGCC)_2$ core, which is present in the primer binding site (PBS) of HIV, offers a possibility for the sequence-selective peptidyl-anthraquinones to be used as drugs acting at early events of HIV replication.[29–31]

Experimental Section

Chemistry

NMR spectra were recorded on a Bruker Avance AMX 300 spectrometer; ^{1}H and ^{13}C NMR spectra were run by using $[D_6]$DMSO as a solvent, and the solvent peak was used as an internal standard. Chemical shifts (δ) are expressed in parts per million (ppm) relative to $(CH_3)_4Si$, and spin multiplicities are indicated as: s (singlet), brs (broad singlet), d (doublet), dd (double doublet), t (triplet), and m (multiplet), and the values are expressed in Hz. Analytical thin-layer chromatography (TLC) was carried out on pre-coated silica gel plates (Merck $60F_{254}$), and spots were visualized with UV light at 254 nm. Preparative column chromatography was performed by using Merck silica gel (230–400 mesh). All starting materials not described below, the solvents and the deuterated solvents were purchased from commercial sources, mainly Aldrich and Fluka. All reagents and solvents were used as received from commercial sources without additional purification, unless stated otherwise. Analytical HPLC was carried out on Varian HPLC system by using a Agilent Extend C_{18} column, 4.6 mm × 250 mm, with a particle size of 5 μm. The mobile phase consisted of A: 0.16 M ammonium formate buffer (70%), pH 2.7 (by formic acid), sodium hexanesulfonate was added at a concentration of 0.025 M as an ion-pair reagent; and B: MeCN; the eluting gradient was: $90_A{:}10_B \rightarrow 10_A{:}90_B$ in 25 min and then $10_A{:}90_B$ for an additional 5 min.[32] The eluate was monitored at 260 nm, an absorption maximum of the anthraquinone nucleus. HRMS data were obtained with a Mariner API-TOF instrument (Perseptive Biosystems Inc., Framingham MA 01701, USA).

1,4-bis[(5-Hydroxypentyl)amino]-9,10-anthracenedione (1): $Na_2S_2O_4$ (1.0 g, 5.7 mmol) was added to a suspension of leucoquinizarin (0.5 g, 2.08 mmol) in 0.5% aq K_2CO_3 (50 mL) under a N_2 atmosphere. The reaction mixture was heated at 100 °C, and $Na_2S_2O_4$ (0.5 g, 2.9 mmol) and the 5-aminopentan-1-ol were added (2.15 g, 20.80 mmol). The reaction mixture was held at reflux overnight, cooled to room temperature, and air was introduced for 6 h under vigorous stirring. H_2O was added until complete precipitation of the product, and the solid was filtered out and dried. The crude product was then purified by column chromatography (EtOAc/MeOH, 9:1) to obtain compound **1** as a blue powder (700 mg, 82%). HPLC: $t_R = 17.7$ min, purity > 99%.[33] ^{1}H NMR (300 MHz, $[D_6]$DMSO): $\delta = 10.92$ (t, $J = 5.3$ Hz, 2H), 8.25 (m, 2H), 7.79 (m, 2H), 7.50 (s, 2H), 4.40 (t, $J = 5.1$ Hz, 2H), 3.49 (m, 8H), 1.70 (m, 4H), 1.50 ppm (m, 8H); ^{13}C NMR (300 MHz, $[D_6]$DMSO): $\delta = 23.5$, 29.5, 32.6, 42.5, 61.0, 108.5, 126.1, 125.1, 132.6, 134.2, 146.5, 180.8 ppm;

HRMS (ES+): *m/z*: calcd for $C_{24}H_{30}N_2O_4$ $[M+H]^+$: 411.5793, found: 411.5145.

1,4-bis{[2-(2-Hydroxyethoxy)ethyl]amino}-9,10-anthracenedione (2): was obtained by using the same procedure as described before by starting from leucoquinizarin (0.5 g, 2.08 mmol) and 2-(2-aminoethoxy)ethanol (2.19 g, 20.80 mmol). The crude product was purified by column chromatography (EtOAc/MeOH, 9:1), to yield compound **2** as a blue powder (800 mg, 93%). HPLC: $t_R = 12.9$ min, purity 99%. ^{1}H NMR (300 MHz, [D$_6$]DMSO): $\delta = 10.88$ (t, $J = 5.2$ Hz, 2H), 8.24 (dd, $J = 2.5$ Hz, $J = 5.9$ Hz, 2H), 7.79 (dd, $J = 2.5$ Hz, $J = 5.9$ Hz, 2H), 7.50 (s, 2H), 4.62 (t, $J = 5.0$ Hz, 2H), 3.71 (t, $J = 5.0$ Hz, 4H), 3.61 (m, 4H), 3.53 ppm (m, 8H); ^{13}C NMR (300 MHz, [D$_6$]DMSO): $\delta = 42.5$, 60.6, 69.6, 72.7, 108.8, 125.0, 126.1, 132.7, 134.2, 146.3, 181.1 ppm; HRMS (ES+): *m/z*: calcd for $C_{22}H_{26}N_2O_6$ $[M+H]^+$: 415.7658, found: 415.7209.

1,4-bis[{2-[(2-Hydroxyethyl)amino]ethyl}amino]-9,10-anthracenedione (3): was obtained by following literature preparation, from 1,4-difluoroanthraquinone (200 mg, 0.819 mmol) in DMSO (4 mL) and *N*-(2-Hydroxyethyl)ethylenediamine (256 mg, 2.457 mmol). Compound **3** was prepared as a blue powder (120 mg, 36%). HPLC: $t_R = 9.4$ min, purity $>99\%$.[34] ^{1}H NMR (300 MHz, [D$_6$]DMSO): $\delta = 10.69$ (t, $J = 6.3$ Hz, 2H), 8.24 (dd, $J = 3.2$ Hz, $J = 5.8$ Hz, 2H), 7.83 (dd, $J = 3.2$ Hz, $J = 5.8$ Hz, 2H), 7.68 (s, 2H), 3.59 (m, 4H), 3.30 (m, 4H), 2.80 ppm (m, 8H); ^{13}C NMR (300 MHz, [D$_6$]DMSO): $\delta = 48.5$, 49.6, 52.5, 62.2, 109.7, 118.7, 129.8, 132.4, 133.8, 138.3, 182.2 ppm; HRMS (ES+): *m/z*: calcd for $C_{22}H_{28}N_4O_4$ $[M+H]^+$: 413.9581, found: 413.9256.

1,4-bis{[5-(Boc-Glycyl)hydroxypentyl]amino}-9,10-anthracenedione (4): *N,N*-Dicyclohexylcarbodiimide (DCC; 25.2 mg, 0.122 mmol), *N,N*-dimethylaminopyridine (DMAP; 14.9 mg, 0.122 mmol) and Boc-Gly-OH (214 mg, 1.22 mmol) were added to a solution of **1** (50 mg, 0.122 mmol) in THF (10 mL) under an argon atmosphere. The reaction mixture was stirred at room temperature overnight. Then the solvent was evaporated under vacuum and the residue was purified by column chromatography (toluene/EtOAc, 8:2), to yield compound **4** as a blue powder (52 mg, 59%). HPLC: $t_R = 28.6$ min, purity $>99\%$. ^{1}H NMR (300 MHz, [D$_6$]DMSO): $\delta = 10.88$ (t, $J = 5.4$ Hz, 2H), 8.25 (dd, $J = 2.5$ Hz, $J = 5.9$ Hz, 2H), 7.78 (dd, $J = 2.5$ Hz, $J = 5.9$ Hz, 2H), 7.50 (s, 2H), 7.20 (t, $J = 6.3$ Hz, 2H), 4.08 (t, $J = 6.3$ Hz, 4H), 3.67 (m, 4H), 3.45 (m, 4H), 1.68 (m, 8H), 1.50 (m, 4H), 1.36 ppm (s, 18H); ^{13}C NMR (300 MHz, [D$_6$][D$_6$]DMSO): $\delta = 23.2$, 28.2, 28.5, 29.2, 42.3, 64.5, 78.6, 108.6, 125.1, 126.1, 132.6, 134.2, 146.4, 156.2, 170.8, 180.9 ppm; HRMS (ES+): *m/z*: calcd for $C_{38}H_{52}N_4O_{10}$ $[M+H]^+$: 725.3534, found: 725.3557.

1,4-bis[{2-[2-(Boc-Glycyl)hydroxyethoxy]ethyl}amino]-9,10-anthracenedione (5): By using the previous procedure from compound **2** (50 mg, 0.122 mmol) and Boc-Gly-OH (214 mg, 1.22 mmol), compound **5** was prepared as a blue powder (73 mg, 82%). HPLC: $t_R = 20.6$ min, purity $>99\%$. ^{1}H NMR (300 MHz, [D$_6$]DMSO): $\delta = 10.87$ (t, $J = 5.2$ Hz, 2H), 8.23 (dd, $J = 2.5$ Hz, $J = 5.9$ Hz, 2H), 7.81 (dd, $J = 2.5$ Hz, $J = 5.9$ Hz, 2H), 7.50 (s, 2H), 7.22 (t, $J = 6.1$ Hz, 2H), 4.25 (m, 4H), 3.92 (t, $J = 6.1$ Hz, 4H), 3.65 (m, 4H), 3.60 (m, 4H), 3.23 (m, 4H), 1.40 ppm (s, 18H); ^{13}C NMR (300 MHz, [D$_6$]DMSO): $\delta = 28.5$, 42.3, 44.0, 64.4, 69.1, 70.3, 79.5, 110.7, 118.7, 130.1, 132.2, 133.7, 138.2, 156.3, 169.6, 182.2 ppm; HRMS (ES+): *m/z*: calcd for $C_{36}H_{48}N_4O_{12}$ $[M+H]^+$: 729.8067, found: 729.3319.

1,4-bis{[2-{[2-(2-Boc-Glycyloxyethyl)]amino}ethyl]amino}-9,10-anthracenedione (6): By using the same procedure described previously for the preparation of compound **4**, and starting from **3** (70 mg, 0.170 mmol) and Boc-Gly-OH (214 mg, 1.22 mmol), compound **6** was obtained as a blue powder (22 mg, 18%). HPLC: $t_R = 16.2$ min, purity 98%. ^{1}H NMR (300 MHz, [D$_6$]DMSO): $\delta = 11.25$ (t, $J = 5.2$ Hz, 2H), 8.25 (s,2H), 7.80 (dd, $J = 2.5$ Hz, $J = 5.9$ Hz, 2H), 7.55 (dd, $J = 2.5$ Hz, $J = 5.9$ Hz, 2H), 6.50 (s, 2H), 4.20 (m, 4H), 3.95 (s, 4H), 3.20 (m, 4H), 2.80 (m, 8H), 1.40 ppm (s, 18H); ^{13}C NMR (300 MHz, [D$_6$]DMSO): $\delta = 28.5$, 42.3, 48.7, 49.5, 64.1, 79.5, 108.9, 125.5, 131.2, 132.7, 134.2, 138.4, 156.3, 169.6, 180.9 ppm; HRMS (ES+): *m/z*: calcd for $C_{36}H_{50}N_6O_{10}$ $[M+H]^+$: 727.8292, found: 727.8990.

1,4-bis{[5-(Glycyl)hydroxypentyl]amino}-9,10-anthracenedione bistrifluoroacetate (7): A solution of **4** (40 mg, 0.055 mmol) in 90% TFA (50 μL) was stirred for 1 h at room temperature and then cold Et_2O (5 mL) was added. The reaction mixture was kept at 0 °C for 30 min and filtered; the precipitate was washed twice with Et_2O (5 mL). Compound **7** was obtained as a blue powder (39 mg, 94%). HPLC: $t_R = 15.7$ min, purity 99%. ^{1}H NMR (300 MHz, [D$_6$]DMSO): $\delta = 10.80$ (t, $J = 5.2$ Hz, 2H), 8.25 (dd, $J = 2.5$ Hz, $J = 5.9$ Hz, 2H), 7.78 (dd, $J = 2.5$ Hz, $J = 5.9$ Hz, 2H), 7.50 (s, 2H), 4.10 (s, 4H), 3.64 (m, 4H), 3.44 (m, 4H), 1.80 (m, 4H), 1.55 ppm (m, 8H); ^{13}C NMR (300 MHz, [D$_6$]DMSO): $\delta = 23.3$, 28.7, 29.9, 39.8, 45.1, 65.0, 108.5, 117.4 (TFA), 125.2, 126.5, 132.7, 134.2, 146.7, 161.4 (TFA), 167.4, 180.9 ppm; HRMS (ES+): *m/z*: calcd for $C_{28}H_{36}N_4O_6$ $[M+2H]^+$: 263.3247, found: 263.3163.

1,4-bis[{2-[2-(Glycyl)hydroxyethoxy]ethyl}amino]-9,10-anthracenedione bistrifluoroacetate (8): With the same procedure described for compound **7**, from **5** (50 mg, 0.069 mmol) in 90% TFA (50 μL), compound **8** was prepared as a blue powder (50 mg, 97%). HPLC: $t_R = 10.9$ min, purity 98%. ^{1}H NMR (300 MHz, [D$_6$]DMSO): $\delta = 10.82$ (t, $J = 5.2$ Hz, 2H), 8.24 (dd, $J = 2.5$ Hz, $J = 5.9$ Hz, 2H), 7.79 (dd, $J = 2.5$ Hz, $J = 5.9$ Hz, 2H), 7.50 (s, 2H), 4.25 (m, 4H), 3.67 (m, 4H), 3.62 (s,4H), 3.58 (m, 4H), 3.23 ppm (m, 4H); ^{13}C NMR (300 MHz, [D$_6$]DMSO): $\delta = 40.9$, 44.8, 64.1, 69.0, 70.2, 109.5, 117.4, 118.2, 129.5, 132.4, 133.7, 138.7, 161.4, 169.6, 182.2 ppm; HRMS (ES+): *m/z*: calcd for $C_{26}H_{32}N_4O_8$ $[M+2H]^+$: 265.1183, found: 265.1156.

1,4-bis{[2-{[2-(2-Glycyloxyethyl)]amino}ethyl]amino}-9,10-anthracenedione bistrifluoroacetate (9): By using the same procedure described for the preparation of compound **7**, and by starting from **6** (20 mg, 0.028 mmol), compound **9** was prepared as a blue powder (18 mg, 85%). HPLC: $t_R = 9.3$ min, purity $>99\%$. ^{1}H NMR (300 MHz, [D$_6$]DMSO): $\delta = 11.25$ (t, $J = 5.3$ Hz, 2H), 8.25 (s, 2H), 7.82 (dd, $J = 2.6$ Hz, $J = 5.8$ Hz, 2H), 7.57 (dd, $J = 2.6$ Hz, $J = 5.8$ Hz, 2H), 6.48 (s, 2H), 4.16 (m, 4H), 3.97 (s, 4H), 3.22 (m,4H), 2.84 ppm (m, 8H); ^{13}C NMR (300 MHz, [D$_6$]DMSO): $\delta = 40.4$, 48.5, 49.7, 64.1, 108.9, 117.4, 125.5, 131.2, 132.7, 134.2, 138.4, 169.6, 171.4, 180.9 ppm, HRMS (ES+): *m/z*: calcd for $C_{26}H_{34}N_6O_6$ $[M+2H]^+$: 264.3654, found: 264.3156.

1,4-bis{[5-(Boc-Lys(Boc)-Glycyl)hydroxypentyl]amino}-9,10-anthracenedione (10): A solution of Boc-Lys-(Boc)-OSu (80 mg, 0.180 mmol) in CH_2Cl_2 (14 mL), which had been adjusted to pH 9 with Et_3N was added to a solution of **7** (31 mg, 0.042 mmol) in DMF (2 mL). The reaction mixture was stirred for 2 h. Then H_2O was added, the product was extracted in CH_2Cl_2, and the organic phase was evaporated under vacuum. The crude product was purified by column chromatography, (EtOAc/MeOH, 9:1), to obtain compound **10** as a blue powder (25 mg, 50%). HPLC: $t_R = 29.6$ min, purity 99%. ^{1}H NMR (300 MHz, [D$_6$]DMSO): $\delta = 10.82$ (t, $J = 5.2$ Hz, 2H), 8.25 (dd, $J = 2.5$ Hz, $J = 5.9$ Hz, 2H), 7.80 (dd, $J = 2.5$ Hz, $J = 5.9$ Hz, 2H), 7.50 (s, 2H), 4.53 (m, 2H), 4.16 (s, 4H), 4.08 (m, 4H), 3.06 (m, 4H), 2.96 (m, 4H), 1.79 (m, 4H), 1.57 (m, 8H), 1.52 (m, 4H), 1.40 (s, 36H), 1.29 ppm (m, 8H); ^{13}C NMR (300 MHz, [D$_6$]DMSO): $\delta = 23.3$, 28.5, 28.7, 29.4, 29.9, 31.5, 40.8, 42.1, 45.1, 55.4, 65.0, 79.7,

108.9, 125.5, 131.2, 132.7, 134.2, 138.4, 156.0, 169.6, 171.4, 180.9 ppm; HRMS (ES+): *m/z*: calcd for $C_{60}H_{92}N_8O_{16}$ $[M+H]^+$: 1181.6572, found: 1181.6617.

1,4-bis[{2-[2-(Boc-Lys(Boc)-Glycyl)hydroxyethoxy]ethyl}amino]-9,10-anthracenedione (11): By using the same procedure described for compound **10**, and by starting from compound **8** (50 mg, 0.066 mmol) and Boc-Lys(Boc)-OSu (88 mg, 0.198 mmol), compound **11** was obtained as a blue powder (36 mg, 46%). HPLC: $t_R = 26.8$ min, purity >99%. ^{1}H NMR (300 MHz, [D$_6$]DMSO): $\delta = 10.82$ (t, $J = 5.2$ Hz, 2H), 8.25 (dd, $J = 2.5$ Hz, $J = 5.9$ Hz, 2H), 7.80 (dd, $J = 2.5$ Hz, $J = 5.9$ Hz, 2H), 7.50 (s, 2H), 4.53 (m, 2H), 4.25 (m, 4H), 4.16 (s, 4H), 3.65 (m, 4H), 3.60 (m, 4H), 3.23 (m, 4H), 2.96 (m, 4H), 1.79 (m, 4H), 1.55 (m, 4H), 1.40 (s, 36H), 1.29 ppm (m, 4H); ^{13}C NMR (300 MHz, [D$_6$]DMSO): $\delta = 20.7$, 28.5, 28.7, 29.4, 31.5, 40.8, 41.9, 44.0, 55.4, 65.0, 69.1, 70.2, 79.7, 108.9, 125.5, 131.2, 132.7, 134.2, 138.4, 156.0, 169.6, 171.4, 180.9 ppm; HRMS (ES+): *m/z*: calcd for $C_{58}H_{88}N_8O_{18}$ $[M+H]^+$: 1185.3995, found: 1185.3756.

1,4-bis{[2-{[2-(2-Boc-Lys(Boc)-Glycyloxyethyl)]amino}ethyl]amino}-9,10-anthracenedione (12): By using the same procedure as described above for compound **10**, and by starting from compound **9** and Boc-Lys-(Boc)-Osu (17 mg, 0.038 mmol), compound **12** was synthesized as a blue powder (21 mg, 93%). HPLC: $t_R =$ 22.1 min, purity >99%.^{1}H NMR (300 MHz, [D$_6$]DMSO): $\delta = 10.82$ (t, $J = 5.2$ Hz, 2H), 8.60 (s, 2H), 8.25 (dd, $J = 2.5$ Hz, $J = 5.9$ Hz, 2H), 7.80 (dd, $J = 2.5$ Hz, $J = 5.9$ Hz, 2H), 6.80 (s, 2H), 4.20 (m, 8H), 3.90 (m, 4H), 3.75 (m, 2H), 3.60 (m, 8H), 2.66 (m, 4H), 1.70 (m, 4H), 1.52 (m, 4H), 1.40 (s, 36H), 1.35 ppm (m, 4H); ^{13}C NMR (300 MHz, [D$_6$]DMSO): $\delta = 21.5$, 28.5, 29.3, 31.5, 40.7, 42.1, 48.5, 49.7, 55.2, 64.3, 79.5, 108.9, 125.5, 131.2, 132.7, 134.2, 138.4, 156.0, 169.6, 171.4, 180.9 ppm; HRMS (ES+): *m/z*: calcd for $C_{58}H_{90}N_{10}O_{16}$ $[M+H]^+$: 1183.4389, found: 1183.4295.

1,4-bis{[5-(Lys-Glycyl)hydroxypentyl]amino}-9,10-anthracenedione tetrafluoroacetate (13): A solution of **10** (20 mg, 0.017 mmol) in 90% TFA (50 μL) was stirred for 1 h at room temperature, then cold Et_2O was added. The reaction mixture was cooled to, and kept at 0 °C for 30 min, and the precipitate was filtered out and washed with cold Et_2O and finally dried. Compound **13** was obtained as a blue powder (17 mg, 81%). HPLC: $t_R =$ 18.7 min, purity 98%. ^{1}H NMR (300 MHz, [D$_6$]DMSO): $\delta = 10.80$ (t, $J = 5.3$ Hz, 2H), 8.25 (dd, $J = 2.5$ Hz, $J = 5.9$ Hz, 2H), 7.78 (dd, $J =$ 2.5 Hz, $J = 5.9$ Hz, 2H), 7.50 (s, 2H), 4.16 (s, 4H), 4.08 (m,4H), 3.56 (s, 2H), 3.06 (m, 4H), 2.65 (m, 4H), 1.79 (m, 4H), 1.55 (m, 8H), 1.50 (m, 4H), 1.28 ppm (m, 8H); ^{13}C NMR (300 MHz, [D$_6$]DMSO): $\delta = 20.7$, 23.3, 28.7, 29.9, 32.1, 34.3, 40.8, 42.3, 45.1, 54.2, 65.0, 108.5, 117.4, 125.2, 126.5, 132.7, 134.2, 138.2, 161.4, 169.4, 171.4, 180.9 ppm; HRMS (ES+): *m/z*: calcd for $C_{40}H_{60}N_8O_8$ $[M+2H]^+$: 391.2340, found: 391.2468.

1,4-bis[{2-[2-(LysGlycyl)hydroxyethoxy]ethyl}amino]-9,10-anthracenedione tetrafluoroacetate (14): By the same procedure described before, from compound **11** (30 mg, 0.025 mmol) compound **14** was obtained as a blue powder (30 mg, 97%). HPLC: $t_R = 13.7$ min, purity 98%. ^{1}H NMR (300 MHz, [D$_6$]DMSO): $\delta = 10.80$ (t, $J = 5.3$ Hz, 2H), 8.25 (dd, $J = 2.5$ Hz, $J = 5.9$ Hz, 2H), 7.78 (dd, $J =$ 2.5 Hz, $J = 5.9$ Hz, 2H), 7.50 (s, 2H), 4.25 (m, 4H), 4.16 (s, 4H), 3.65 (m,4H), 3.60 (m, 4H), 3.56 (m, 2H), 3.26 (m, 4H), 2.65 (m, 4H), 1.79 (m, 4H), 1.55 (m, 4H), 1.29 ppm (m, 4H); ^{13}C NMR (300 MHz, [D$_6$]DMSO): $\delta = 20.7$, 32.1, 34.3, 40.8, 42.1, 44.0, 54.1, 64.4, 69.1, 70.3, 108.5, 117.4, 125.2, 126.5, 132.7, 134.2, 138.2, 161.4, 169.4, 171.4, 180.9 ppm; HRMS (ES+): *m/z*: calcd for $C_{38}H_{56}N_8O_{10}$ $[M+H]^+$: 785.4114, found: 785.4154.

1,4-bis{[2-{[2-(2-Lys-Glycyloxyethyl)]amino}ethyl]amino}-9,10-anthracenedione tetrafluoroacetate (15): By the same procedure described before, from compound **12** (20 mg, 0.017 mmol) product **15** as a blue powder was obtained (17 mg, 81%). HPLC: $t_R =$ 11.7 min, purity >99%. ^{1}H NMR (300 MHz, [D$_6$]DMSO): $\delta = 10.80$ (t, $J = 5.3$ Hz, 2H), 8.62 (s, 2H), 8.20 (dd, $J = 2.5$ Hz, $J = 5.9$ Hz, 2H), 7.78 (dd, $J = 2.5$ Hz, $J = 5.9$ Hz, 2H), 6.75 (s, 2H), 4.20 (m, 8H), 3.92 (m, 4H), 3.80 (m, 2H), 3.60 (m, 8H), 2.67 (m, 4H), 1.74 (m, 4H), 1.50 (m, 4H), 1.36 ppm (s, 4H); ^{13}C NMR (300 MHz, [D$_6$]DMSO): $\delta = 21.5$, 29.3, 31.5, 40.7, 42.1, 48.5, 49.7, 55.2, 64.3, 108.9, 117.2, 125.5, 131.2, 132.7, 134.2, 138.4, 161.4, 169.6, 171.4, 180.9 ppm; HRMS (ES+): *m/z*: calcd for $C_{38}H_{58}N_{10}O_8$ $[M+2H]^+$: 392.2292, found: 392.2385.

1,4-bis{[2-{[2-(2-Boc-Glycyloxyethyl)]Boc-Gly-amino}ethyl]amino}-9,10-anthracenedione (16): DCC (30 mg, 0.146 mmol), DMAP (18 mg, 0.146 mmol), and Boc-Gly-OH (128 mg, 0.73 mmol) were added to a solution of **3** (30 mg, 0.073 mmol) in THF (10 mL), under an argon atmosphere. The reaction mixture was stirred at room temperature overnight, the solvent was evaporated under vacuum, and the residue was purified by column chromatography (EtOAc/MeOH, 95:5), to obtain compound **16** as a blue powder (25 mg, 33%). HPLC: $t_R = 16.8$ min, purity >99%. ^{1}H NMR (300 MHz, [D$_6$]DMSO): $\delta = 10.95$ (t, $J = 5.2$ Hz, 2H), 7.85 (dd, $J = 2.5$ Hz, $J =$ 5.9 Hz, 2H), 7.65 (dd, $J = 2.5$ Hz, $J = 5.9$ Hz, 2H), 6.70 (s, 2H), 4.30 (m, 4H), 3.92 (s, 4H), 3.85 (s, 4H), 3.48 (m, 8H), 3.32 (s, 4H), 1.38 ppm (s, 36H); ^{13}C NMR (300 MHz, [D$_6$]DMSO): $\delta = 28.6$, 42.5, 46.4, 46.8, 47.5, 61.5, 79.5, 108.9, 125.5, 131.2, 132.7, 134.2, 138.4, 156.3, 164.3, 169.8, 181.1 ppm; HRMS (ES+): *m/z*: calcd for $C_{50}H_{72}N_8O_{16}$ $[M+H]^+$: 1041.5066, found: 1041.4940.

1,4-bis{[2-{[2-(2-Glycyloxyethyl)]Gly-amino}ethyl]amino}-9,10-anthracenedione tetrafluoroacetate (17): A solution of **16** (25 mg, 0.024 mmol) in 90% TFA (50 μL) was stirred for 1 h at room temperature, and then cold Et_2O was added. The reaction mixture was cooled and held at 0 °C for 30 min, and the precipitate was filtered off and dried to furnish compound **17** as a blue powder (14 mg, 91%). HPLC: $t_R = 9.2$ min, purity 98%. ^{1}H NMR (300 MHz, [D$_6$]DMSO): $\delta = 11.25$ (t, $J = 5.3$ Hz, 2H), 7.90 (dd, $J = 2.6$ Hz, $J =$ 5.8 Hz, 2H), 7.84 (dd, $J = 2.6$ Hz, $J = 5.8$ Hz, 2H), 6.58 (s, 2H), 4.36 (m, 4H), 3.62 (s, 4H), 3.54 (s, 4H), 3.48 (m, 4H), 3.43 (m, 4H), 3.25 ppm (m, 4H); ^{13}C NMR (300 MHz, [D$_6$]DMSO): $\delta = 40.4$, 41.5, 46.3, 46.7, 47.8, 61.4, 108.9, 117.4, 125.5, 131.2, 132.7, 134.2, 138.4, 164.5, 169.8, 171.4, 181.0 ppm; HRMS (ES+): *m/z*: calcd for $C_{30}H_{40}N_8O_8$ $[M+2H]^+$: 321.2985, found: 321.2529.

Compound solutions

Stock anthraquinones solutions were prepared in anhyd DMSO. All compounds were characterized spectrophotometrically and fluorimetrically. They presented similar absorbance profiles relative to the parental drug, ametantrone (**3**). Concentrations of solutions were therefore obtained by using the experimentally calculated molar absorption coefficient of ametantrone, 5400 $M^{-1}cm^{-1}$ at 626 nm, 25 °C in deionized purified (Milli-Q) H_2O.

Unwinding assays

This assay was chosen to evaluate anthraquinones intercalating activity and possible unwinding of the double helix. Briefly, 0.25 μg supercoiled pBR322 plasmid (MBI Fermentas), was incubated in increasing quantity of the test compound into a final volume of 20 μL in Tris 10 mM, EDTA 1 mM at pH 8 (TE buffer). After 1 h incubation time, all samples were loaded into a 1% agarose gel and

run overnight at 15 V cm^{-1} in TBE (89 mM Tris, 89 mM boric acid, 2 mM EDTA, pH 8.0). To obtain the open circular (OC) form, the pBR322 plasmid was incubated in ice for 5 min with 0.001 U μL^{-1} RQ1 DNase-RNase-free (Promega) in 40 mM Tris-HCl pH 8.0, 10 mM $MgSO_4$ and 1 mM $CaCl_2$. Nicking was stopped by adding 20 mM EGTA, pH 8.0 (Promega). Linearization of plasmid was performed by digestion with EcoRI (Fermentas) as indicated by the supplier. Agarose (supplied by BioRad) gels were poured at a 1% concentration and run in TBE buffer 1× (89 mM Tris, 89 mM boric acid, 20 mM EDTA). Ethidium bromide (Sigma) stocks at 10 mg mL^{-1} were diluted to 50 μg mL^{-1} in deionized purified (Milli-Q) H_2O and added to visualize the DNA after electrophoresis.

Melting assays

The determination of the melting temperatures of double-stranded oligonucleotides of known sequences was determined by fluorescence quenching (FQA) essentially as described.[25] Briefly, three pairs of different oligonucleotides were used: each pair was labeled at the 5′ end of the forward strand with the FRET probe FAM (6′-carboxyfluorescein), and with DAB (dabcyl, *N*-4′-carboxy-4-(dimethylamino)azobenzene) at the 3′ end of the reverse strand. FAM is a fluorescent molecule characterized by a high quantum yield, with maximum emission wavelength at 517 nm when excited at 494 nm ($\varepsilon_{494} = 83\,000$ cm^{-1} M^{-1}), efficiently quenched by DAB.[35] The random sequence was obtained annealing FAM–GTG AGA TAC CGA CAG AGG (FAM-random) with CCT CTG TCG TGA TCT CAC–DAB (DAB-random); the second and the third pairs were specific sequences whose core was designed according to theoretical studies,[17,18] namely Z1 by annealing FAM–5′-ACT ATT CCC GGG TAA TGA-3′ (FAM-Z1) with 5′-TCA TTA CCC GGG TAA AGT-3′–DAB (DAB-Z1). FAM–5′-ACT ATT GGC GCC TAA TGA-3′ (FAM-Z2) and 5′-TCA TTA GGC GCC AAT AGT-3′–DAB (DAB-Z2) oligonucleotide were annealed to give the Z2 oligo. FQA was carried out in capillary glasses in a Roche Light Cycler 1.5, and the software allowed us to collect and analyze all the data. The variation of T_m (ΔT_m) was the parameter chosen to describe different blunt-ended hybrid oligonucleotide's stability over the temperature increase. It was calculated by monitoring the variation of fluorescence with the temperature. The inflexion point of the melting profile of the double-stranded oligonucleotide that was derived by the software, gave the T_m for each melting profile. Oligonucleotides solutions were prepared by dissolving the lyophilized nucleic acids in a proper TE volume to obtain 1 mM concentrated stock solution. Their concentration was determined by UV measurement at 260 nm. Melting reactions took place into glass capillaries containing the incubation mixture (20 μL): anthraquinones (2 μL) at a final concentration of 1, 10, and 100 μM; HB buffer (4 μL; HB 20: 10 mM Tris, 1 mM EDTA, 20 mM NaCl, pH 7.5). Before the assay took place, forward and reverse strand oligo solutions were mixed at equimolar concentrations, denatured at 95 °C for 5 min, and allowed to anneal at room temperature for 3 h. Thermal protocol of melting was a ramp 30°–95 °C modified by 1 °C min^{-1} by the light cycler apparatus. The fluorescence in each capillary was read at 520 nm by the same apparatus.

Topoisomerase II-mediated DNA relaxation

For each sample, supercoiled pBR322 plasmid (100 ng; Fermentas) was incubated with increasing concentrations (up to 100 μM) of the test compounds and with the positive control at a final volume of 20 μL in 40 mM Tris-HCl, pH 7.5, 80 mM KCl, 5 mM DTT, 15 ng μL^{-1} BSA, 1 mM ATP and 10 mM $MgCl_2$. Topoisomerase IIα (0.01 U) was added to the + topo II samples. After 1 h incubation at 37 °C, reactions were stopped by adding 0.2 M NaCl, 0.025% bromophenol blue, 5% glycerol (4 μL), loaded into a 1% agarose gel, and run overnight at 15 V cm^{-1} in TBE (89 mM Tris, 89 mM boric acid, 2 mM EDTA, pH 8.0). Gels were stained with ethidium bromide after running (post-staining). Pictures were taken by using the imaging system Geliance 600 (PerkinElmer).

Cytotoxicity

The human HL60 cell line was maintained in RPMI 1640 medium supplemented with 10% heat-inactivated fetal bovine serum (FBS), penicillin (100 U mL^{-1}), and streptomycin (100 μg mL^{-1}). LoVo cells were maintained in F-12 HAM medium supplemented with 10% heat-inactivated FBS, 1% glutamine, penicillin (100 U), and streptomycin (100 μg mL^{-1}). The HeLa cell line was maintained in DMEM supplemented with 10% heat-inactivated FBS, penicillin (100 U mL^{-1}), and streptomycin (100 μg mL^{-1}). The cytotoxicity of the compounds was measured by the colorimetric 3-(4,5-dimethylthiazol-2-yl)-2,5-diphenyltetrazolium bromide (MTT) assay. Briefly, cells (5×10^3 well^{-1}) were cultured in triplicate in a 96-well plate in the absence or presence of various concentrations of the test compounds. After the indicated time of incubation at 37 °C, MTT was added to each well, and the mixture was incubated for 4 h. The medium was removed before addition of DMSO for another 30 min. The plates were then read at 540 nm with a Microplate Reader (BioRad).

Log P

Octanol–water partition coefficient (log *P*) values were determined for each compound by the shake flask method. Peptidyl-anthraquinones were dissolved at known concentrations in a solution of buffer at pH 7.4 (10 mM Tris, 20 mM NaCl, 1 mM $Mg(ClO_4)_2$) saturated with octanol, mixed with an equal amount of buffer-saturated octanol, shaken extensively and allowed to equilibrate over 16 h at room temperature. The UV absorbance of the aqueous solution was measured before and after being shaken. Log *P* was calculated as the log of the ratio of the concentration in the octanol phase to the concentration in the aqueous phase at pH 7.4.

Computational methodologies

All modeling studies were carried out on a 20 CPU (Intel Core2 Quad CPU 2.40 GHz) Linux cluster.

Structure building: Peptidyl-anthraquinone structures were built using the "Builder" module of Molecular Operation Environment (MOE, version 2008.10).[36] The software package MOPAC (version 7),[37] implemented in MOE suite, was used for the structure optimization process by using the HF/PM3 semiempirical method. MOPAC software has been also used to calculate atomic charges by fitting to electrostatic potential maps (EPS method).[37]

Duplex intercalation site preparation: the present study involved the use of consensus dinucleotide intercalation geometry d(CpG) initially obtained by using NAMOT2 software (*Nucleic Acid MOdeling Tool*, Los Alamos National Laboratory, Los Alamos NM, USA).[38] The d(CpG) intercalation site was contained in the center of a hexanucleotide duplex of sequence d(5′-GGCGCC-3′). Hexamers in the B-form were built by using the "DNA Builder" module of Molecular Operation Environment (MOE, version 2008.10).[36] The hexanucleotide was minimized by using the Amber95 all-atom force field,[39]

implemented by MOE modeling package, until the RMS value of Truncated Newton method (TN) was < 0.1 kcal mol^{-1} Å^{-1}. To model the effects of solvent more directly, a set of electrostatic interaction corrections was used. The MOE suite implemented a modified version of GB/SA contact function described by Still and co-authors.[40] These terms model the electrostatic contribution to the free energy of solvation in a continuum solvent model.

Molecular docking protocol: Peptidyl-anthraquinones were docked into both intercalation sites by using the flexible MOE-Dock methodology. The purpose of MOE-Dock is to search for favorable binding configurations between a small, flexible ligand and a rigid macromolecular target. Searching is conducted within a user-specified 3D docking box, by using the "tabù search" protocol[41] and MMFF94 force field.[42] Charges for peptidyl-anthraquinones were imported from the MOPAC output files. MOE-Dock performs a user-specified number of independent docking runs (55 in the presented case) and writes the resulting conformations and their energies to a molecular database file. The resulting DNA–peptidyl-anthraquinone complexes were subjected to MMFF94 all-atom energy minimization until the RMS of conjugate gradient was < 0.1 kcal mol^{-1} Å^{-1}. GB/SA approximation has been used to model the electrostatic contribution to the free energy of solvation in a continuum solvent model.

Molecular dynamics calculation: Peptidyl-anthraquinones were immersed in a rectangular box filled with TIP3P[43] by imposing a minimum solute-wall box distance of 10 Å. The system was neutralized with Na^+ cations by using the AMBER leap module.[44] Each system was modeled by using the AMBER95 all-atom force field[39] with periodic boundary conditions. A cutoff radius of 9 Å was used for nonbonded interactions by updating the neighbor pair list every 10 steps. The electrostatic interactions were calculated with the Particle mesh Ewald method.[45] The SHAKE algorithm[46] was used to constrain all bond lengths involving hydrogen. Optimization and relaxation of solvent and ions were initially performed while keeping the solute atoms constrained to their initial position with decreasing force constants of 500, 25, 15, and 5 kcal mol^{-1} Å^2. Thereafter the system was minimized without any constraints and warmed up. A 2 ns simulation was carried out. In the production phase, the simulation was run with the isothermal-isobaric ensemble (300 K and one atmosphere pressure), and pressure and temperature were maintained by the Berendsen coupling algorithm[47] with a 2 fs time step. Pressure and temperature coupling constants were 0.5 ps. During the production run, from 0.5 to 2 ns, the atom coordinates were saved every 0.1 ps for analysis. The MOE "Conformational Geometry" module was used to check some structural properties (root-mean-square deviation (RMSD), hydrogen bond). Interaction energies are calculated for the entire trajectory by using the MMFF94 force field.

Acknowledgements

This investigation was supported by the MIUR (PRIN, Rome, Italy), AIRC (Associazione Italiana per la Ricerca sul Cancro), and the University of Padova. S.M. is also very grateful to Chemical Computing Group for the scientific and technical partnership.

Keywords: ametantrone conjugates · DNA recognition · drug design · molecular docking · molecular dynamics

[1] A. P. Krapcho, Z. Getahun, K. L. Avery, Jr., K. J. Vargas, M. P. Hacker, S. Spinelli, G. Pezzoni, C. Manzotti, *J. Med. Chem.* **1991**, *34*, 2373 – 2380.
[2] N. A. Cornbleet, R. C. Stuart-Harris, I. E. Smith, E. E. Coleman, R. D. Rubens, M. McDonald, H. T. Mouridsen, H. Rainer, A. T. van Oosterom, J. F. Smyth, *Eur. J. Cancer Clin. Oncol.* **1984**, *20*, 1141 – 1146.
[3] K. Reszka, J. A. Hartley, P. Kolodziejczyk, J. W. Lown, *Biochem. Pharmacol.* **1989**, *38*, 4253 – 4260.
[4] C. Panousis, A. J. Kettle, D. R. Phillips, *Anti-Cancer Drug Des.* **1995**, *10*, 593 – 605.
[5] J. Kapuscinski, Z. Darzynkiewicz, *Biochem. Pharmacol.* **1985**, *34*, 4203 – 4213.
[6] K. X. Chen, N. Gresh, B. Pullmann, *Nucleic Acids Res.* **1986**, *14*, 9103 – 9115.
[7] F. Traganos, *Pharmacol. Ther.* **1983**, *22*, 199 – 214.
[8] W. W. Au, M. A. Butler, T. S. Matney, T. L. Loo, *Cancer Res.* **1981**, *41*, 376 – 379.
[9] R. K. Zee-Cheng, C. C. Cheng, *Drugs Future* **1983**, *8*, 229 – 248.
[10] G. Palù, M. Palumbo, G. A. Antonello, S. Marciani-Magno, *Mol. Pharmacol.* **1986**, *29*, 211 – 217.
[11] M. Palumbo, G. Palù, O. Gia, E. Ferrazzi, G. A. Meloni, *Anti-Cancer Drug Des.* **1987**, *1*, 337 – 346.
[12] G. Zagotto, E. Uriarte, C. Antonello, M. T. Conconi, S. Marciani-Magno, *Bioorg. Med. Chem. Lett.* **1992**, *2*, 659 – 662.
[13] B. Gatto, G. Zagotto, C. Sissi, C. Cera, E. Uriarte, G. Palù, G. Capranico, M. Palumbo, *J. Med. Chem.* **1996**, *39*, 3114 – 3122.
[14] B. Gatto, G. Zagotto, C. Sissi, M. Palumbo, *Int. J. Biol. Macromol.* **1997**, *21*, 319 – 326.
[15] G. Zagotto, S. Moro, E. Uriarte, E. Ferrazzi, G. Palù, M. Palumbo, *Anti-Cancer Drug Des.* **1997**, *12*, 99 – 112.
[16] G. Zagotto, R. Supino, E. Favini, S. Moro, M. Palumbo, *Farmaco* **2000**, *55*, 1 – 5.
[17] N. Gresh, P. H. Kahn, *J. Biomol. Struct. Dyn.* **1991**, *8*, 827 – 846.
[18] N. Gresh, P. H. Kahn, *J. Biomol. Struct. Dyn.* **1990**, *7*, 1141 – 1160.
[19] S. Mohammadi, M. Perrée-Fauvet, N. Gresh, K. Hillairet, E. Taillandier, *Biochemistry* **1998**, *37*, 6165 – 6178.
[20] S. Far, A. Kossanyi, C. Verchère-Béaur, N. Gresh, E. Taillandier, M. Perrée-Fauvet, *Eur. J. Org. Chem.* **2004**, *2004*, 1781 – 1797.
[21] S. Wain-Hobson, P. Sonigo, O. Danos, S. Cole, M. Alizon, *Cell* **1985**, *40*, 9 – 17.
[22] L. Ratner, R. C. Gallo, F. Wong-Staal, *Nature* **1985**, *313*, 636 – 637.
[23] F. E. Durr in *Anthracycline and Anthracenedione-Based Anticancer Agents, Vol. 6* (Ed.: W. Lown), Elsevier, New York, **1988**, pp. 401 – 405.
[24] R. K. Zee-Cheng, C. C. Cheng, *J. Med. Chem.* **1978**, *21*, 291 – 294.
[25] B. Gatto, G. Giaretta, M. Bertuzzi, E. Bianchini, G. Zagotto, M. Palumbo in *New Perspectives In Medicinal Chemistry, Vol. 1* (Ed.: S. Alcaro), Research Signpost, Kerala, India, **2009**, pp. 199 – 211.
[26] B. Gatto, O. Tabarrini, S. Massari, G. Giaretta, S. Sabatini, C. Del Vecchio, C. Parolin, A. Fravolini, M. Palumbo, V. Cecchetti, *ChemMedChem* **2009**, *4*, 935 – 938.
[27] M. G. Zagorski, J. U. Bowie, A. K. Vershon, R. T. Sauer, D. J. Patel, *Biochemistry* **1989**, *28*, 9813 – 9825.
[28] J. N. Breg, R. Boelens, A. V. George, R. Kaptein, *Biochemistry* **1989**, *28*, 9826 – 9833.
[29] J. R. Thomas, P. J. Hergenrother, *Chem. Rev.* **2008**, *108*, 1171 – 1224.
[30] B. D. Gooch, P. A. Beal, *J. Am. Chem. Soc.* **2004**, *126*, 10603 – 10610.
[31] J. A. Thomas, R. J. Gorelick, *Virus Res.* **2008**, *134*, 39 – 63.
[32] J. Johnson, A. Ahmad, S. Khan, Y.-F. Wang, A. Abu-Qare, J. Ayoub, A. Zhang, I. Ahmad, *J. Chromatogr. B* **2004**, *799*, 149 – 155.
[33] V. Gibson, R. J. Anderson, T. C. Jenkins, D. Cairns, *Pharmacy Pharmacol. Commun.* **1999**, *5*, 669 – 671.
[34] C. C. Cheng, R. K. Zee-Cheng, *Prog. Med. Chem.* **1983**, *20*, 83 – 118.
[35] S. Tyagi, D. Bratu, F. Kramer, *Nat. Biotechnol.* **1998**, *16*, 49 – 53.
[36] Molecular Operating Environment (MOE) v. 2008.10: Chemical Computing Group Inc., 010 Sherbrooke Street West, Suite 910, Montreal, QC, H3A 2R7 (Canada).
[37] MOPAC 7, J. J. P. Stewart, Fujitsu Ltd.: Tokyo (Japan), **1993**.
[38] E. S. I. Carter, C. S. Tung, *Comput. Appl. Biosci.* **1996**, *12*, 25 – 30.
[39] W. D. Cornell, P. Cieplak, I. Bayly, I. R. Gould, K. M. Merz, Jr., D. M. Ferguson, D. C. Spellmeyer, T. Fox, J. W. Caldwell, P. A. Kollman, *J. Am. Chem. Soc.* **1995**, *117*, 5179 – 5197.

[40] D. Qiu, P. S. Shenkin, F. P. Hollinger, W. C. Still, *J. Phys. Chem. A* **1997**, *101*, 3005 – 3014.
[41] C. A. Baxter, C. W. Murray, D. E. Clark, D. R. Westhead, M. D. Eldridge, *Proteins Struct. Funct. Genet.* **1998**, *33*, 367 – 382.
[42] T. Halgren, *J. Comput. Chem.* **1996**, *17*, 490 – 519.
[43] W. L. Jorgensen, J. Chandrasekhar, J. D. Madura, R. W. Impey, M. L. Klein, *J. Chem. Phys.* **1983**, *79*, 926 – 935.
[44] D. A. Pearlman, D. A. Case, J. W. Caldwell, W. S. Ross, T. E. Cheatham, S. Debolt, D. M. Ferguson, G. Seibel, P. A. Kollman, *Comp. Phys. Commun.* **1995**, *91*, 1 – 41.
[45] T. Darden, D. York, L. Pedersen, *J. Chem. Phys.* **1993**, *98*, 10089 – 10092.
[46] J. P. Ryckaert, G. Ciccotti, H. J. C. Berendsen, *J. Comp. Phys.* **1977**, *23*, 327 – 341.
[47] H. J. C. Berendsen, J. P. M. Postma, W. F. Van Gunsteren, A. Dinola, J. R. Haak, *J. Chem. Phys.* **1984**, *81*, 3684 – 3690.

Received: March 15, 2010
Revised: March 22, 2010
Published online on May 10, 2010

